

Interaction of *S*-polarized beams with infinitely conducting grooves: Enhanced fields and dips in the reflectivity

A. Zuniga-Segundo and O. Mata-Mendez

*Departamento de Fisica, Instituto Politecnico Nacional, Escuela Superior de Fisica y Matematicas,
07738 Zacatenco, Distrito Federal, Mexico*

(Received 15 April 1992)

Field enhancement and reflectivity of *S*-polarized Hermite-Gaussian beams from a rectangular groove ruled on a planar, perfectly conducting surface are analyzed by use of a modal theory. We show a novel effect in which *S* resonances are manifested by the appearance of sharp dips in the scattered intensity. We propose a relationship for the location of these minima in the scattered intensity with a precision better than 10^{-3} .

During the last few years in solid-state physics, great interest has grown regarding the relationship between Raman scattering and surface polaritons.¹⁻³ By now, it is widely accepted that excitation of surface polaritons (which enhances the local-field intensity near the metal surface) is the main origin of surface-enhanced Raman scattering (SERS). This fact has motivated the study of the electric field near surface irregularities; a review is given in Ref. 4. Although *S*-polarized surface polaritons are not known to exist in nonmagnetic materials, it is interesting to investigate whether field enhancement is present with this polarization. Recently, in solid-state physics, infinitely conducting gratings have received attention because it was found theoretically that a silver grating gives practically the same results as for a perfectly conducting grating.⁵⁻⁷ Wirgin and Maradudin⁶ treated an infinitely conducting lamellar grating, obtaining significant electric-field enhancements. However, they did not find any trace of *S* resonances in the far-field intensity, as occur with *P*-polarized radiation. This last negative result had already been presented by Andrewartha, Fox, and Wilson⁸ some years before.

In this paper we present exact numerical calculations for the interaction of *S*-polarized beam waves of finite cross section with one groove ruled on a flat perfectly conducting screen. As incident beams of finite cross section we consider Hermite-Gaussian beams of arbitrary order,^{9,10} where the lowest order is an ordinary Gaussian beam.^{11,12} As was pointed out by Marcuse,¹³ these beams are very important since laser modes have the shape of Hermite-Gaussian functions. To our knowledge, beams of finite cross section have not yet been considered in the study of the electric-field enhancement (*S* or *P* polarization).⁴ Our numerical experiments show that the proximity to *S*-resonant wavelengths is indicated by dips in the reflected intensity, suggesting a simple and practical method for the location of these *S* resonances. It is important to remark that these observed minima in the far-field intensity are not related to any absorption of energy; in fact, a redistribution of energy takes place. We also propose a relationship for the location of these dips in the scattered intensity with a precision better than 10^{-3} .

The geometry of our system is shown in Fig. 1. We consider a rectangular groove ruled on a flat perfectly con-

ducting screen, with width l and thickness h . The screen is placed in vacuum and the position of a point in space is given by its Cartesian coordinates x , y , and z . The rectangular groove is illuminated by an electromagnetic beam wave of finite cross section which is independent of the z coordinate. The complex representation of field quantities is used and the complex time factor $\exp(-i\omega t)$ is omitted in what follows. In this paper we consider only *S*-polarized waves, i.e., E_z is the only component of the electric field and must be null at the interfaces. The total field E must satisfy the Helmholtz equation.⁴ For the sake of simplicity we distinguish three regions, denoted as region 1 ($y > h/2$), region 2 ($-h/2 < y < h/2$), and region 3 ($y < -h/2$), as illustrated in Fig. 1. In region 1, the field $E_1(x, y)$ has the form⁴

$$E_1(x, y) = \frac{1}{(2\pi)^{1/2}} \int_{-k}^{+k} A(\alpha) e^{i(\alpha x - \beta y)} d\alpha + \frac{1}{(2\pi)^{1/2}} \int_{-\infty}^{+\infty} B(\alpha) e^{i(\alpha x + \beta y)} d\alpha, \quad (1)$$

where $\alpha^2 + \beta^2 = k^2$, with β or β/i positive and $ck = \omega$. If

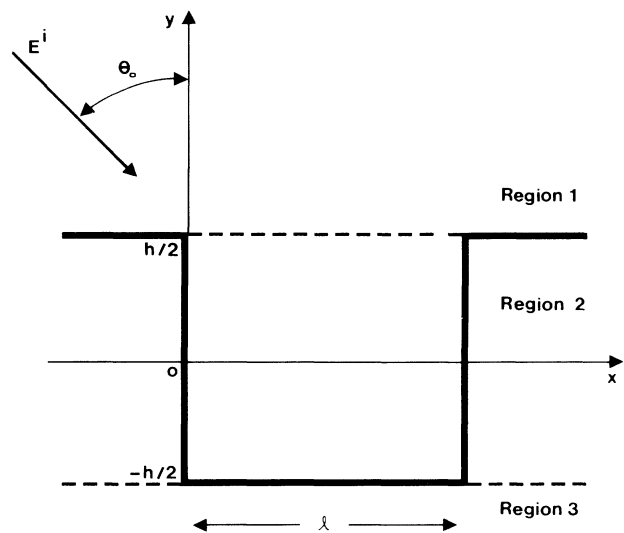


FIG. 1. Configuration of the system. θ_0 is the angle of incidence. The z axis is perpendicular to the figure.

the first integral of Eq. (1) is identified with the incident field E' , this solution satisfies the radiation condition (or the outgoing wave radiation). In region 2, we can represent E_2 by the following modal expansion:

$$E_2(x, y) = \sum_{n=1}^{\infty} [a_n \cos(\mu_n y) + b_n \sin(\mu_n y)] \phi_n(x), \quad (2)$$

where $\mu_n^2 = k^2 - n^2 \pi^2 / l^2$, with μ_n or μ_n / i positive. The functions $\phi_n(x)$ are given by

$$\phi_n(x) = \begin{cases} \sin(n\pi x / l), & 0 \leq x \leq l, \\ 0, & \text{elsewhere.} \end{cases} \quad (3)$$

This expansion is in accord with the fact that E_2 must be null inside a perfectly conducting metal. Finally, in region 3, we have the condition $E_3(x, y) = 0$. Our problem is to determine the amplitude $B(\alpha)$ of the scattered field [Eq. (1)] and the modal coefficients a_n and b_n of Eq. (2), when the amplitude $A(\alpha)$ of the incident beam wave is known.

The requirement that the tangential component of the electric field must be continuous at $y = -h/2$ results in

$$a_n = b_n \tan(\mu_n h / 2). \quad (4)$$

The other boundary conditions, continuity of E and $\partial E / \partial y$ at $y = h/2$ and across the slit at $y = h/2$, respectively, led us to the following system of equations in b_n :

$$\sum_{n=1}^{\infty} M_{mn} b_n + N_m b_m = S_m, \quad (5)$$

where M_{mn} , N_m , and S_m are given by

$$M_{mn} = 2i \sin(\mu_n h / 2) \langle \beta(\alpha) \hat{\phi}_n(\alpha), \hat{\phi}_m(\alpha) \rangle, \quad (6)$$

$$N_m = -\frac{\mu_m l \cos(\mu_m h)}{2 \cos(\mu_m h / 2)}, \quad (7)$$

$$S_m = 2i \langle \beta(\alpha) A(\alpha) e^{-i\beta h / 2}, \hat{\phi}_m(\alpha) \rangle. \quad (8)$$

$\hat{\phi}_n(\alpha)$ is the Fourier transform of $\phi_n(x)$. We have the notation

$$\langle f(\alpha), g(\alpha) \rangle = \int_{-\infty}^{+\infty} f(\alpha) g(\alpha)^* d\alpha. \quad (9)$$

By solving Eq. (5), the coefficients b_n are determined, these b_n substituted into Eq. (4) allow the determination of the coefficients a_n , and the solution for the problem is formally obtained. Using Eqs. (2) and (4) we can write down the field within the groove in terms of a_n or b_n :

$$\begin{aligned} E_2(x, y) &= \sum_{n=1}^{\infty} [\tan(\mu_n h / 2) \cos(\mu_n y) + \sin(\mu_n y)] \phi_n(x) b_n \\ &= \sum_{n=1}^{\infty} [\cos(\mu_n y) + \cot(\mu_n h / 2) \sin(\mu_n y)] \phi_n(x) a_n. \end{aligned} \quad (10)$$

We are naturally interested in determining conditions of existence of cavity resonances and methods to detect these resonances. To our knowledge no study has been carried out in these directions for no-periodical structures with S -polarized waves. The most important contributions have been given for gratings.⁶ A closer look at Eq. (10) gives immediately the following conditions for the electric-field enhancement within the grooves:

$$\tan(\mu_n h / 2) = \pm \infty \text{ or } \cot(\mu_n h / 2) = \pm \infty, \quad (11)$$

where μ_n has been defined below Eq. (2). We find that for the wavelengths λ , solutions of these equations are

$$\lambda_{nm} = 2 \left(\frac{n^2}{l^2} + \frac{m^2}{h^2} \right)^{-1/2}, \quad (12)$$

$$m = 1, 2, 3, 4, \dots, \quad n = 1, 2, 3, 4, \dots$$

This is a relationship between the wavelength λ_{nm} and the groove dimensions (the width l and the thickness h). We notice the important fact that Eq. (12) is independent of the incident beam wave. It is easy to verify from Eq. (12) that $\lambda_{nm} < \lambda_c$, where $\lambda_c = 2l$ is the cutoff wavelength for the associated waveguide obtained when h is infinite, so that, in resonant condition the scattered field penetrates deep into the groove reaching the bottom.^{11,14} In order to understand the nature of the S resonances, let us consider a two-dimensional rectangular resonant cavity, whose dimensions are l and h . The Helmholtz equation plus the boundary condition $E_z = 0$ form an eigenvalue problem. We find that the normal wavelengths of this closed cavity are identical with the resonant wavelengths given by Eq. (12). We think that this kind of analogy will be very useful in considering more complicated configurations, for instance, rough surfaces.⁴

Studies of resonant conditions for gratings (S -polarized light) have been done by several authors. A critical review of these papers was done by Wirgin and Maradudin in Ref. 6. In that paper, it was treated as an infinitely conducting lamellar grating and, in their Eq. (10), an expression for the location of cavity resonances was proposed. It is not hard to see that our Eq. (12), with $n=1$, reduces to that proposed by Wirgin and Maradudin. This result shows that one rectangular groove has more S resonances than a lamellar grating. Our numerical experiments (and those of Ref. 6) show that the actual resonant wavelengths λ are very close to those calculated with Eq. (12).

As an incident beam, we consider the two-dimensional version of the field distribution of a Hermite-Gaussian beam. The amplitude $A(\alpha)$ of the incident beam [see Eq. (1)] is given by^{9,10,13}

$$A(\alpha) = L/2(i)^m H_m[-(\alpha \cos \theta_0 - \beta \sin \theta_0)L/8^{1/2}] (\cos \theta_0 + \alpha/\beta \sin \theta_0) e^{i(-\alpha b + \beta h/2)} \exp[-(\alpha \cos \theta_0 - \beta \sin \theta_0)^2 L^2/8], \quad (13)$$

where $L/2$ is the local $1/e$ intensity beam radius, related to the $1/e$ field beam radius $a/2$ by $L = a/2^{1/2}$. We locate the beam waist on the screen at $x=b$ and $y=h/2$, where b will be taken as $l/2$ from now on, i.e., the Hermite-Gaussian beam will be centered on the slit at $y=h/2$. H_m denotes the Hermite polynomial of order m and θ_0 is the

angle of incidence of the limited beam (Fig. 1). As was pointed out by Marcuse,¹³ these beams are very important since laser modes have the shape of Hermite-Gaussian functions. As far as we know, this is the first time where incident Hermite-Gaussian beams are considered in the calculation of enhanced electric field near surfaces. We

find, for Gaussian beams ($m=0$), significant field enhancements comparable to those of Wirgin and Maradudin (for a conducting lamellar grating) given in Figs. 3 and 4 of Ref. 6. Besides the fundamental beam ($m=0$), we have treated incident Hermite-Gaussian beams of order $m \neq 0$, but no significant field enhancements were found. In these last calculations ($m \neq 0$), the minima of the incident beam were not considered avoiding very large fictitious enhancements of the order of 10^9 .

We now turn to the following interesting question: How is the resonant enhancement of the electric field within the groove related to the observed reflectivity? In other words, how will the S resonances be detected? First Andrewartha, Fox, and Wilson⁸ and later Wirgin and Maradudin⁶ gave a negative answer to this question in the case of periodical objects (gratings). They did not find any trace of S resonances in the far-field intensity. However, from our calculations we show that the S resonances can be detected from the observed reflectivity for non-periodical objects (one or two grooves).

The differential reflection coefficient (dR) is defined as the fraction of the energy in the incident beam which is scattered into the angular interval $(\theta, \theta + d\theta)$. Figure 2 displays the typical behavior of the scattered intensities when one is close to a resonant wavelength. The logarithm of $dR/d\theta$ as a function of the scattering angle θ , for a Gaussian beam normally incident on a groove $0.35 \mu\text{m}$ wide by $1 \mu\text{m}$ deep, at various wavelengths is shown. In this figure, the proximity to the resonant wavelength $\lambda_{21} = 0.3447 \mu\text{m}$ is indicated by two symmetrical dips in the reflected intensity. The reader will notice that when λ

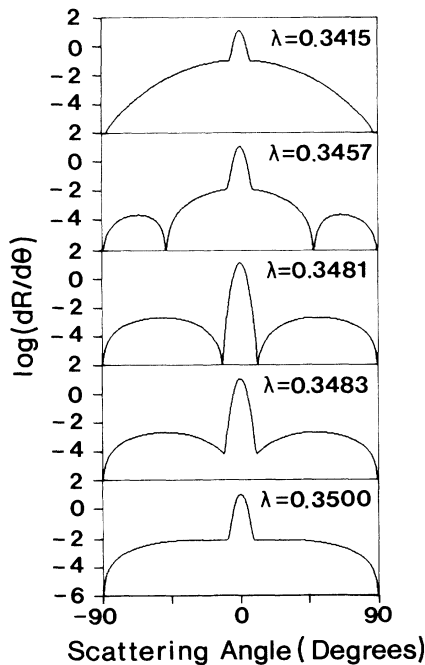


FIG. 2. Typical behavior of the scattered intensities when one is close to a resonant wavelength, showing the collapse of dip pairs close to $\theta = \pm 0^\circ$. The logarithm of $dR/d\theta$ for a normally incident Gaussian beam is displayed at various wavelengths. $L = 3/2^{1/2} \mu\text{m}$, $h = 1.0 \mu\text{m}$, and $l = 0.35 \mu\text{m}$.

goes from below, through, and then above the resonant wavelength λ_{21} , the dip pairs move from $\theta = \pm 90^\circ$ to lower θ values, collapsing finally close to $\theta = \pm 0^\circ$. In this last example, $L/l = 6.06$, if $L/l \gg 1$ the collapse takes place very close to $\theta = \pm 0^\circ$. This novel and sensitive effect occurs in a very narrow range of wavelengths ($\Delta\lambda \approx \lambda/100$) that include the resonance value, suggesting simple and practical ways for determining S resonances. One way to use this "resonance dip-pair collapse effect" (RDPCE) to detect S resonances is described below.

Let $dR/d\theta$ be measured by varying λ at a fixed scattering angle θ ; dips will be observed due to the resonant enhancement of the electric field within the groove. From the numerical point of view, these dips and those of the RDPCE (Fig. 2) can be observed easily; however, the most favorable experimental conditions in which to detect these dips are obtained when the incident spot size l is of the order of the groove width l with $L > l$. An example of the appearance of these dips is displayed in Fig. 3, when a Gaussian beam ($L/l = 6.06$) is normally incident on the groove mentioned above and λ varies in the interval $0.29\text{--}0.79 \mu\text{m}$. The fixed scattering angle θ is 30° . It follows from Eq. (12) that nine resonances may be predicted at $\lambda_{11} = 0.6607 \mu\text{m}$, $\lambda_{12} = 0.5734 \mu\text{m}$, $\lambda_{13} = 0.4827 \mu\text{m}$, $\lambda_{14} = 0.4068 \mu\text{m}$, $\lambda_{15} = 0.3472 \mu\text{m}$, $\lambda_{16} = 0.3009 \mu\text{m}$, $\lambda_{21} = 0.3447 \mu\text{m}$, $\lambda_{22} = 0.3303 \mu\text{m}$, and $\lambda_{23} = 0.3098 \mu\text{m}$. From Fig. 3, however, only six dips are detected. How can the other three missing resonances be detected? The answer to this question is given by Fig. 4, where the fundamental incident beam has been replaced by a Hermite-Gaussian beam of odd order ($m=1$). The three missing dips are clearly shown. In Table I we list the resonant wavelengths λ_{nm} calculated from Eq. (12), along with the dips λ_i ($i=1, \dots, 9$) observed in Figs. 3 and 4. Let us note that with other fixed scattering angles θ the same λ_i 's were found. Thus, we find that our simple relationship equation (12) is able to locate the dips observed in the scattered intensity with a precision better than 10^{-3} . This novel effect (RDPCE) and Eq. (12) could be applied

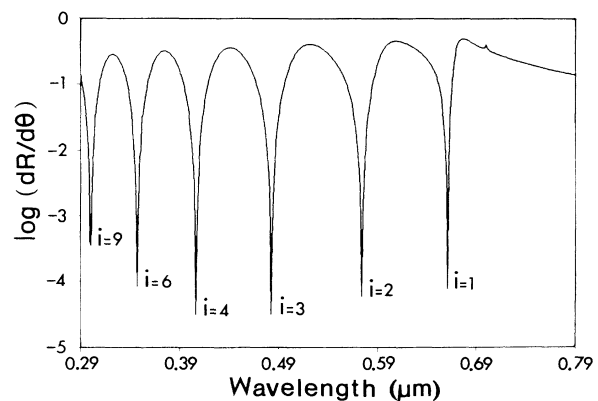


FIG. 3. Logarithm of the differential reflection coefficient per unit angle $d\theta$ ($dR/d\theta$) as a function of wavelength for a fixed scattering angle ($\theta = 30^\circ$). A normally incident Gaussian beam is considered. Six resonant wavelengths denoted by λ_i ($i = 1, 2, 3, 4, 6, \text{ and } 9$) are labeled in the figure. $L = 3/2^{1/2} \mu\text{m}$, $h = 1.0 \mu\text{m}$, and $l = 0.35 \mu\text{m}$.

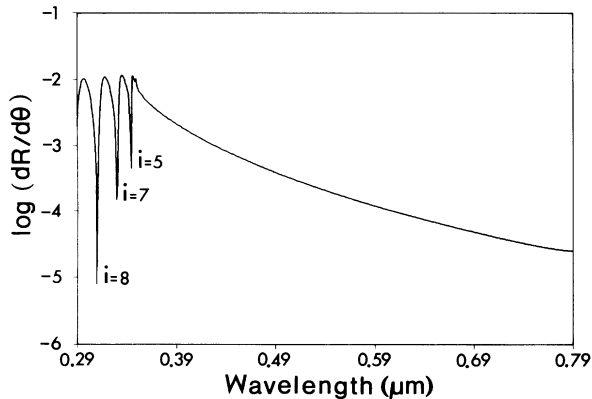


FIG. 4. The same as Fig. 3 but for a normally incident Hermite-Gaussian beam of order $m=1$. Three resonant wavelengths denoted by λ_i ($i=5, 7$, and 8) are labeled in the figure.

to a number of interesting practical problems; for instance, they can be used as a sensitive wavelength selector. The groove depth can be determined by scattered light measurements; this is an inverse scattering problem.¹⁴ These results can also be used for characterizing the properties of rough surfaces.⁴

In conclusion, we have presented exact numerical calculations for the interaction of S -polarized Hermite-Gaussian beams with one groove ruled on a flat perfectly conducting screen. We have demonstrated a novel effect (RDPCE) in which S resonances are manifested by the appearance of sharp dips in the scattered intensity. In ad-

TABLE I. Comparison between the resonant wavelengths λ_{nm} (calculated) and the resonant wavelengths λ_i (observed).

λ_{nm} (μm) (calculated)	λ_i (μm) (observed)
$\lambda_{11}=0.6607$	$\lambda_1=0.6608$
$\lambda_{12}=0.5734$	$\lambda_2=0.5737$
$\lambda_{13}=0.4827$	$\lambda_3=0.4830$
$\lambda_{14}=0.4068$	$\lambda_4=0.4068$
$\lambda_{15}=0.3472$	$\lambda_5=0.3469$
$\lambda_{21}=0.3447$	$\lambda_6=0.3447$
$\lambda_{22}=0.3303$	$\lambda_7=0.3304$
$\lambda_{23}=0.3098$	$\lambda_8=0.3100$
$\lambda_{16}=0.3009$	$\lambda_9=0.2999$

dition, we have proposed a simple way to experimentally detect S resonances and a relationship [Eq. (12)] that gives their location with a precision better than 10^{-3} . These results suggest a practical way for determining cavity-type resonances, i.e., they provide favorable experimental conditions in order to obtain, for instance, a large SERS signal or a large response of nonlinear materials. We expect that the effect predicted will stimulate the experimental work in these directions.

The authors acknowledge support from COFAA-IPN (Mexico) and CONACYT (Mexico). We also wish to thank R. Fajardo-Castaneda (UAM-Mexico) for computational assistance.

¹Surface-Enhanced Raman Scattering, edited by R. K. Chang and T. E. Furtak (Plenum, New York, 1982).

²Y. J. Chen, E. Burstein, and D. L. Mills, Phys. Rev. Lett. **34**, 1516 (1975).

³Martin Moskovits, Rev. Mod. Phys. **57**, 783 (1985).

⁴O. Mata-Mendez, Phys. Rev. B **37**, 8182 (1988).

⁵P. Sheng, R. Stepleman, and P. Sanda, Phys. Rev. B **26**, 2907 (1982).

⁶A. Wirgin and A. A. Maradudin, Phys. Rev. B **31**, 5573 (1985).

⁷D. Maystre, M. Nevriere, and R. Petit, in *Electromagnetic Theory of Gratings*, edited by R. Petit, Topics in Current Physics Vol. 22 (Springer-Verlag, Berlin, 1980), p. 159.

⁸J. R. Andrewartha, J. R. Fox, and I. J. Wilson, Opt. Acta **26**, 69 (1979).

⁹Toshitaka Kojima, J. Opt. Soc. Am. A **7**, 1740 (1990).

¹⁰Takato Kudou, Mitsuhiro Yokota, and Otozo Fukumitsu, J. Opt. Soc. Am. A **8**, 718 (1991).

¹¹O. Mata-Mendez, M. Cadilhac, and R. Petit, J. Opt. Soc. Am. **73**, 328 (1983).

¹²O. Mata-Mendez, Opt. Lett. **16**, 1629 (1991).

¹³Dietrich Marcuse, *Light Transmission Optics* (Van Nostrand, New York, 1975), Chap. 6.

¹⁴O. Mata-Mendez, A. Roger, and D. Maystre, Appl. Phys. B **32**, 199 (1983).